

Modelling of carbon diffusion and ferritic phase transformations in an unalloyed hypoeutectoid steel

M. WOLFF ¹⁾, C. ACHT ²⁾, M. BÖHM ¹⁾, S. MEIER ¹⁾

¹⁾*Zentrum für Technomathematik
Fachbereich 3, University of Bremen
D-28334 Bremen, Germany*

²⁾*Stiftung Institut für Werkstofftechnik
Bremen, Germany*

DURING THE IMPORTANT industrial process of case hardening, phase transformations in a steel workpiece are essentially influenced by the (non-homogeneous) carbon distribution (near the surface). Moreover, the temperature course is of great importance. We develop a mathematical model of case hardening which takes diffusion of carbon in austenite, heat conduction and possible phase transformations into account. In this work, mechanical behaviour (thermo-elasticity, classical plasticity and transformation-induced plasticity) is not included in the model. As a result we obtain an initial-boundary-value problem for a coupled system of two parabolic partial and several ordinary differential equations. Finally, we present some numerical simulations.

Key words: mathematical modelling, steel, case hardening, carbon diffusion, phase transformations, system of PDEs and ODEs.

1. Introduction

IT IS THE AIM of this work to model carbon diffusion in steel on a macroscopic level, in interaction with ferritic phase transformations and heat conduction. This situation occurs, for instance, during the industrial process of carburisation of steel workpieces followed by quenching (so-called case hardening), but also during phase transformations in steel workpieces with a given inhomogeneous carbon distribution. We refer, for instance, to the recent engineering articles [1, 2, 5, 27, 41] dealing with carburisation and case hardening. It is well known that carburisation and quenching happen on different time scales. Particularly for large workpieces with a high case-hardening depth, the carburisation process can take several hours [27]. Since carbon diffusion is heavily temperature-dependent, an increase in temperature from 950° C to 1050° C can reduce the carburisation time by half. When carrying out such high-temperature carburi-

sation, an isothermal phase transformation is often enforced after the carburisation and before the quenching in order to guarantee a sufficiently fine-grained microstructure (cf. [27] and references therein). For discussions concerning the material properties of steel, phase transformations and heat treatment we refer to [3, 7, 8, 11–13, 18, 22, 26, 28, 31, 36], e.g.

In our model of diffusion, heat conduction and phase transformations, we obtain a coupled system consisting of two parabolic partial differential equations for carbon diffusion in austenite and for heat conduction and of several ordinary differential equations accounting for the phase transformations.

Although this paper is especially concerned with case hardening, our approach is also applicable to more general situations where diffusion and phase transformations play a role. Besides this, decarburisation before quenching, when the edge layer releases carbon to the environment, can also be captured by the model proposed here. We emphasise that in this work *macroscopic* models are considered. In particular, we do not dwell on the meso- and microstructure of steel and its phases. Keywords in this context are grains and grain boundaries or local carbon diffusion during the formation of ferrite and pearlite. All quantities such as phase fractions and mass fractions refer to averages over not-too-small volumes (so-called *representative volume elements (RVEs)*, cf. [6, 15, 17, 52]). A more detailed model accounting for diffusion on the meso-scale would require additional notions and equations. Corresponding remarks are given below. Unlike the earlier work [47], some assumptions in the present paper are less restrictive (cf. the specific assumptions regarding the course of the phase transformations in Sec. 3.2).

Generally, phase transformations may lead to mechanical deformations of the workpiece. In order to focus, we do not include mechanical behaviour (e.g. thermo-elasticity, transformation-induced plasticity (TRIP), plasticity) in the model. This remains for future work. The distortion of workpieces related to carburisation and case hardening is investigated in [1, 2, 26, 27]. Numerical computations with the commercial software SYSWELD[®] can be found in [1, 2]. For general models of the material behaviour of steel including phase transformations and TRIP we refer to [26] and, without carbon diffusion, to [39, 44, 45, 48].

In Sec. 2, basic assumptions are formulated concerning the involved phenomena such as carbon diffusion in austenite, heat conduction and phase transformations in steel. We derive a rather general model of phase transformations that includes several known approaches. Afterwards, in Sec. 3, the specific phase transformations of austenite that occur in unalloyed hypoeutectoid steel are described. After this, the entire mathematical model is recapitulated in Sec. 4. In Sec. 5 we present some numerical simulations with realistic data. Finally, in Sec. 6 we give some remarks on how to take mechanical behaviour and grain size into account.

2. Macroscopic modelling – basics

2.1. Phenomenological assumptions

In order to fix ideas, we make the following assumptions:

1. We develop a *macroscopic model*. This means that steel is considered as a co-existing mixture of its phases, which do not diffuse but rather stay at the position where they are formed (cf. [44, 45, 48], e.g.). The meso-scale is only considered as far as it seems necessary for the macroscopic description. The choice of phases occurring in the model is mostly made by macroscopic considerations. For instance, pearlite is regarded as one phase although it is actually a mixture of ferrite and cementite.
2. We restrict ourselves to ferritic phase transformations, i.e., when the process starts, only austenite is present, which transforms under certain conditions into the different ferritic phases. The reverse transformations are *not* considered except that of ferrite into austenite above the eutectoid temperature. This seems reasonable since during quenching processes, the temperature decreases rapidly and a possible re-warming due to the latent heats generally plays a minor role. Moreover, transformations between austenite and ferrite before quenching, which are important in practical applications (cf. [27], e.g.), are included.
3. Since only a small amount of carbon is dissolved in ferrite, we consider *only* carbon diffusion in austenite and not in the ferritic phases. The mesoscopic diffusion of carbon, for instance during the formation of pearlite, does not appear in the macroscopic model equations since pearlite is regarded as one phase. When a ferritic phase is formed, the associated carbon can no longer diffuse through the austenite.
4. In the heat equation, only sources and sinks due to the phase transformations are taken into account. Moreover, cross-diffusion effects between carbon and heat transport (cf. [24], e.g.) are neglected since they are not relevant in steel.
5. The phase transformations strongly depend on temperature and carbon content (cf. Sec. 2.4). In order to reduce the number of possible phases it seems appropriate to assume certain ranges of temperature and carbon content that are not exceeded. The possible phases are then determined with the help of the corresponding iron-carbon diagram (see [7, 8, 22, 33, 36], e.g.). We restrict ourselves to the hypoeutectoid regime and to unalloyed steels (cf. Sec. 3).
6. Since the densities of the phases in steel differ only a little (for fixed temperature), we do not distinguish between mass and volume fractions of the phases (cf. [43]). Although this simplification is usually made, it should be

noted that the small differences in the phase densities can cause distortion of steel workpieces. In carburisation, the changes in density are an important source of distortion (cf. [1]).

7. In order to focus, in this work, mechanical deformations are neglected except for some comments in Sec. 6. Therefore, distortion, in particular that related to case hardening, can not be described by the proposed model. However, the composition of the phases and accordingly, the hardness of the material can be predicted. In order to capture the distortion effects, it is necessary to add a momentum balance as well as additional constitutive equations (e.g., thermo-elasticity with phase transformations, TRIP, or classical plasticity) to the model. This remains for future research. For modelling of mechanical behaviour of steel including carbon diffusion, phase transformations, TRIP and classical plasticity, we refer to [26], as well as to [4, 13, 15, 20, 21, 31, 39, 44–46, 48] (without carbon diffusion) and the literature cited therein.

2.2. Modelling of carbon diffusion in austenite

We consider diffusion in a solid body subject to small deformations and in which the change of a fixed volume as well as its mass by diffusion is negligible. In case of large deformations, the corresponding Piola transformation has to be applied (cf. [19, 51], e.g.). It is assumed that $N \geq 2$ phases are relevant where austenite has always index 1. Let us consider a representative volume element (RVE) V at a point $x \in \Omega$, where the (three-dimensional) domain Ω represents the workpiece. The mass of carbon existing in V and dissolved in phase i ($i = 1, \dots, N$) is denoted by m_{ci} . Then we define the mass concentration (= partial density) of carbon dissolved in phase i referring to the total volume V in x , at time t , by

$$(2.1) \quad c_{ci}(x, t) := \frac{1}{V} \int_V \tilde{\rho}_{ci}(x, t, y) \gamma_i(x, t, y) dy, \quad i = 1, \dots, N,$$

where γ_i is the characteristic function of phase i in V and $\tilde{\rho}_{ci}$ is the microscopic (mesoscopic) mass concentration (partial density) of carbon in phase i . Accordingly, the volume fraction p_i and the mass fraction ψ_i of phase i are defined as

$$(2.2) \quad p_i(x, t) := \frac{1}{V} \int_V \gamma_i(x, t, y) dy, \quad i = 1, \dots, N,$$

$$(2.3) \quad \psi_i(x, t) := \frac{\rho_i(x, t)}{\rho(x, t)} dy, \quad i = 1, \dots, N,$$

where ρ is the mass density of the RVE and ρ_i is the mass density of phase i in V . Of course, the sum of all c_{ci} is then equal to the total mass concentration of the carbon in the workpiece. Let J_{c1} be the diffusion flux density of carbon in austenite (*referring to the total volume*). Then the diffusion equation

$$(2.4) \quad \frac{\partial c_{c1}}{\partial t} + \operatorname{div} J_{c1} = f \quad \text{in } \Omega \times]0, T[$$

is valid, where f is a source which is specified below and $T > 0$ is the duration time of the process. By assumption 3 in 2.1, carbon can only diffuse in austenite. Therefore, the following variant of Fick's law is appropriate:

$$(2.5) \quad J_{c1} = -d_{c1}(\theta)p_1 \nabla \left(\frac{c_{c1}}{p_1} \right).$$

Here, d_{ci} is the temperature-dependent diffusion coefficient of carbon in austenite. The presence of the volume fraction p_1 under the gradient can be motivated by the following argument: Assume that c_{ci} is constant in space, but p_1 is non-constant. Since in this case the carbon concentration in austenite can not be constant, diffusion will occur. The volume fraction in front of the gradient indicates that diffusion can happen only in austenite. Equation (2.5) reads then as follows:

$$(2.6) \quad \frac{\partial c_{c1}}{\partial t} - \operatorname{div} \left(d_{c1}(\theta)p_1 \nabla \left(\frac{c_{c1}}{p_1} \right) \right) = f \quad \text{in } \Omega \times]0, T[.$$

Now we specify f . When a phase, say, ferrite, is built up from austenite, the carbon located in this phase does no longer diffuse through the austenite. Since in our setting the ferritic phases can only be built up from and transform into austenite, we have

$$(2.7) \quad f = - \sum_{j=2}^N \frac{\partial c_{cj}}{\partial t}.$$

The sign in (2.7) is negative because a growth of phase j leads to a decrease of carbon mass in austenite (*referring to the total volume*). We remark that without carbon diffusion from (2.6) and (2.7) the relation

$$(2.8) \quad \sum_{j=1}^N \frac{\partial c_{cj}}{\partial t} = 0$$

follows, which means that the total carbon concentration can only change due to (macroscopic) diffusion. Alternatively, we can express the quantities c_{cj} by

the mass fraction of carbon u_{cj} ($:=$ quotient of masses) in phase j and by the mass fraction ψ_j of phase j (referring to total mass). From the definitions of these quantities one obtains easily

$$(2.9) \quad c_{cj} = \rho u_{cj} \psi_j.$$

Hence, from (2.7) and (2.9) it follows for the source term

$$(2.10) \quad f = -\rho \sum_{j=2}^N \frac{\partial}{\partial t} (u_{cj} \psi_j).$$

Due to (2.9), the relation (2.10) is valid also for a non-constant total density ρ . In this case, a standard argument on time derivatives of particular volume integrals has to be used (cf. [19, 51], e.g.). Summarising (2.6) and (2.10), we obtain an inhomogeneous diffusion equation for c_{c1} :

$$(2.11) \quad \frac{\partial c_{c1}}{\partial t} - \operatorname{div} \left(d_{c1}(\theta) p_1 \nabla \left(\frac{c_{c1}}{p_1} \right) \right) = -\rho \sum_{j=2}^N \frac{\partial}{\partial t} (u_{cj} \psi_j) \quad \text{in } \Omega \times]0, T[.$$

By assumption 7 in 2.1 we do not distinguish between mass and volume fractions of a phase in steel. Therefore, we assume approximately

$$(2.12) \quad p_j = \psi_j,$$

and refer only to the *phase fraction* p_j . In order to model the appropriate boundary conditions, we proceed as follows. By the general theory of mixtures, in equilibrium the chemical potentials of carbon in steel and carbon in the surrounding medium coincide at the boundary. We do not specify them here but refer to [34]. What is important here is the fact that they are functions of carbon concentration and of temperature. Therefore we assume on that part of the boundary where carbon can diffuse,

$$(2.13) \quad \mu_{c\Gamma}(c_{c\Gamma}, \theta) = \mu_c \left(\frac{c_{c1}}{p_1}, \theta \right).$$

In (2.13) $\mu_{c\Gamma}$ and μ_c are the corresponding chemical potentials of carbon in the surrounding medium and in steel, respectively. And $c_{c\Gamma}$ is the ambient mass concentration, i.e., the mass of carbon per volume of the surrounding medium. In general, $\mu_{c\Gamma}$ depends on how carbon is given in the carburisation medium. For the non-equilibrium case we obtain a (generally nonlinear) Robin boundary condition if we assume that the diffusion flux along the normal is proportional

to the difference of the chemical potentials. This reads

$$(2.14) \quad J_{c1} \mathbf{v} = -d_{c1}(\theta)p_1 \frac{\partial}{\partial \mathbf{v}} \left(\frac{c_{c1}}{p_1} \right) = \delta_{c1}(\theta)p_1 \left(\mu_c \left(\frac{c_{c1}}{p_1}, \theta \right) - \mu_{c\Gamma}(c_{c\Gamma}, \theta_\Gamma) \right) \\ \text{at } \partial\Omega \times]0, T[.$$

Here we have used: \mathbf{v} – unit normal vector to $\partial\Omega$ directed outwards, δ_{c1} – temperature- and space-dependent mass-transfer coefficient for carbon in austenite, θ_Γ – ambient temperature. At those parts of the boundary where no exchange happens, we set δ_{c1} equal to zero. The initial condition is

$$(2.15) \quad c_{c1}(x, 0) = c_{c10}(x) \quad \text{for } x \in \Omega$$

with the initial concentration c_{c10} . Instead of the quantity c_{c1} , the mass fraction of carbon in austenite is often employed. Thanks to (2.9), (2.12), and the constancy of the density ρ we obtain from (2.11) (note also (2.7))

$$(2.16) \quad \frac{\partial}{\partial t}(p_1 u_{c1}) - \text{div}(d_{c1}(\theta)p_1 \nabla(u_{c1})) = - \sum_{j=2}^N \frac{\partial}{\partial t}(u_{c_j} p_j) = - \frac{1}{\rho} \sum_{j=2}^N \frac{\partial c_{c_j}}{\partial t} \\ \text{in } \Omega \times]0, T[.$$

Depending on the situation, we will work with both representations of the source term. The relation (2.9) yields also the boundary conditions for u_{c1} , namely, instead of (2.13)

$$(2.17) \quad -d_{c1}(\theta) \frac{\partial}{\partial \mathbf{v}}(u_{c1}) = \frac{\delta_{c1}(\theta)}{\rho} (\mu_c(\rho u_{c1}, \theta) - \mu_{c\Gamma}(c_{c\Gamma}, \theta_\Gamma)) \quad \text{at } \partial\Omega \times]0, T[.$$

It is possible to linearise the difference of the potentials (cf. [34], e.g.), by setting approximately $\theta = \theta_\Gamma$. In this case, one obtains instead of (2.17) a Robin boundary condition being linear in u_{c1}

$$(2.18) \quad -d_{c1}(\theta) \frac{\partial}{\partial \mathbf{v}}(u_{c1}) = \delta_{c1}(\theta) \mu_c^0(\theta) \left(u_{c1} - \frac{c_{c\Gamma}}{\rho} \right) \quad \text{at } \partial\Omega \times]0, T[,$$

where μ_c^0 is a temperature-dependent parameter. Relation (2.9) leads to the initial condition

$$(2.19) \quad u_{c1}(x, 0) = u_{c10}(x).$$

REMARK 1. For convenience, we use the carbon concentration as the primary variable instead of a thermodynamic potential. Besides this, the Henry coefficient is taken equal to one.

(i) Assume that no (macroscopic) diffusion of carbon in austenite happens and hence, by assumption 3 in 2.1, no diffusion in steel happens at all. Then it follows from (2.16) that

$$(2.20) \quad \sum_{j=1}^N \frac{\partial}{\partial t} (u_{cj} p_j) = 0.$$

From (2.20) we can recover the so-called lever rule (cf. [7, 8], e.g.) for the total mass fraction u of carbon in steel

$$(2.21) \quad \sum_{j=1}^N u_{cj} p_j = u(x) \quad \text{for } x \in \Omega.$$

In case of a homogeneous carbon distribution u is constant also with respect to x .

(ii) Frequently, additional quantities are defined in order to relate the macro to the micro-(meso) scale. For instance, in contrast to (2.1),

$$(2.22) \quad \rho_{ci}(x, t) := \left(\int_V \gamma_i(x, t, y) dy \right)^{-1} \int_V \tilde{\rho}_{ci}(x, t, y) \gamma_i(x, t, y) dy$$

denotes the mass concentration (= partial density) of carbon dissolved in phase i , referring to the part of V occupied by phase i (intrinsic phase average of $(\tilde{\rho}_c)$). Then it is clear that

$$(2.23) \quad \rho_{ci} = \frac{c_{ci}}{p_i}.$$

We refer to [6, 14, 15, 41] for further discussions.

(iii) If carbon diffusion in the other phases needs to be taken into account, then a diffusion equation analogous to (2.6) has to be employed for each c_{ci} :

$$(2.24) \quad \frac{\partial c_{ci}}{\partial t} - \operatorname{div} \left(d_{ci}(\theta) p_i \nabla \left(\frac{c_{ci}}{p_i} \right) \right) = f_i \quad i = 1, \dots, N \quad \text{in } \Omega \times]0, T[.$$

If, in contrast to assumption 2 in 2.1, we would admit all transformations $i \rightarrow j$ ($i \neq j$), then we can associate a carbon sink $-f_{ij}$ ($f_{ij} \geq 0$) (from the viewpoint of i) to each transformation. In this case, the right-hand side f_i in (2.24) reads:

$$(2.25) \quad f_i = - \sum_{j=1, j \neq i}^N f_{ij} + \sum_{j=1, j \neq i}^N f_{ji}.$$

The f_{ij} for the particular transformations need to be determined from additional considerations (e.g., from the iron-carbon diagram, see Fig. 1, and, for instance, [22, 33, 36]). The sum of the f_i from 1 to N has to be zero for consistency with the conservation of mass. From (2.24), it follows that the quantity

$$(2.26) \quad \mathbf{J} := \sum_{j=1}^N d_{ci}(\theta) p_i \nabla \left(\frac{c_{ci}}{p_i} \right)$$

can be regarded as flux density of carbon diffusion through the bulk material. The model (2.24), (2.25) is able to describe much more general situations than those considered in this work, namely, diffusion of a (low-concentrated) substance through a mixture or a material undergoing phase transformations. If necessary, one has to distinguish between mass and volume fractions of the different phases.

(iv) In engineering applications, percentage of the mass fractions u_{ci} is often used for calculations instead of the mass fractions itself. Therefore, if necessary, the above equations as well as the initial and boundary conditions need to be modified by multiplying u_{ci} by the factor 100.

2.3. Modelling of heat conduction

We consider now the heat equation in connection with carbon diffusion in austenite and phase transformations. For the temperature θ , we employ the parabolic Eq. (cf. [19, 44, 45, 48]) (\mathbf{u}_c stands for (u_{c1}, \dots, u_{cN}))

$$(2.27) \quad \rho c_e \theta' - \operatorname{div}(\kappa \nabla \theta) = \rho \sum_{i=2}^N L_i(\mathbf{u}_c, \theta) p_i', \quad \text{in } \Omega \times]0, T[.$$

For the sake of brevity, from now on, the time derivatives (ordinary as well as partial) are also denoted by a prime. The quantities in (2.27) are: ρ – density in reference configuration (by assumption 2 in 2.1, this coincides with the density of austenite at initial temperature θ_0 and initial concentration of carbon in austenite u_{c10}), c_e – specific heat, κ – heat conductivity, L_i – latent heat associated to the transformation of austenite into phase i ($i = 2, \dots, N$). For κ and c_e we adopt a rule of mixtures which is linear with respect to the phase fractions:

$$(2.28) \quad c_e(\mathbf{u}_c, \theta, \mathbf{p}) := \sum_{i=1}^N c_{ei}(u_{ci}, \theta) p_i,$$

$$(2.29) \quad \kappa(\mathbf{u}_c, \theta, \mathbf{p}) := \sum_{i=1}^N \kappa_i(u_{ci}, \theta) p_i.$$

(\mathbf{p} stands for (p_1, p_2, \dots, p_N)). We choose the following initial and boundary conditions:

$$(2.30) \quad \theta(x, 0) = \theta_0(x) \quad \text{in } \Omega,$$

$$(2.31) \quad -\kappa(\mathbf{u}_c, \theta, \mathbf{p}) \frac{\partial \theta}{\partial \mathbf{v}} = \delta_\theta(\mathbf{u}_c, \theta, \mathbf{p})(\theta - \theta_\Gamma) \quad \text{at } \partial\Omega \times]0, T[,$$

where θ_0 denotes the initial temperature, θ_Γ – the ambient temperature and δ_θ – the heat-transfer coefficient which in general has to be computed by a rule of mixture analogous to (2.28), (2.29).

2.4. Modelling of phase transformations – a general approach

Using suggestions for multi-phase modelling of phase transformations in [16, 29, 30, 38], we choose a rather general modelling approach which includes several known ones (see [4, 20, 21, 49], e.g.) As an advantage of this procedure, we do not need to fix *prior* a particular transformation law such as that of Johnson–Mehl–Avrami or that of Leblond–Devaux (see also Remark 2 and [9–12, 23, 29–31] and references therein). Moreover, the concretions for our situation will be specified later. We assume that $N \geq 2$ phases are distinguished for the process that needs to be modelled (e.g., quenching of a hypoeutectoid steel workpiece). Then the phase fractions p_j satisfy the general balance as well as non-negativity conditions:

$$(2.32) \quad \sum_{i=1}^N p_i(x, t) = 1 \quad \text{in } \Omega \times]0, T[,$$

$$(2.33) \quad p_i(x, t) \geq 0 \quad \text{for } i = 1, \dots, N \quad \text{in } \Omega \times]0, T[.$$

Let us assume, that the transformation of the i -th phase into the j -th phase ($i \neq j$), abbreviated as $i \rightarrow j$, has its transformation rate $-a_{ij}$, i.e., for the transformation $i \rightarrow j$ (for $i, j = 1, \dots, N, i \neq j$) the change of p_i for p_j can be described by the transformation law

$$(2.34) \quad p'_i = -a_{ij}.$$

In accordance with (2.34) the growth of p_j at expense of p_i is expressed as

$$(2.35) \quad p'_j = a_{ij}.$$

As a consequence of (2.34), (2.35), we set

$$(2.36) \quad a_{ii} := 0 \quad i = 1, \dots, N$$

and

$$(2.37) \quad a_{ij} \geq 0 \quad i, j = 1, \dots, N.$$

Clearly, in case of impossibility of the transformation $i \rightarrow j$ we have $a_{ij} = 0$, too. Here, we let the a_{ij} depend on θ, \mathbf{u}_c , but, generally, they can depend on further variables (cf. [46, 49] e.g.). Based on experimental experience, we assume for phase transformations *in steel* (cf. [9, 29–31] and references therein):

$$(2.38) \quad \text{For } i, j \in \{1, \dots, N\} \text{ with } i \neq j, \text{ there exists a value } \bar{p}_{ij} = \bar{p}_{ij}(\theta, \mathbf{u}_c) \text{ (} k \neq i, j \text{), such that the phase transformation } p_i \rightarrow p_j \text{ is only possible if } p_i > 0 \text{ and } \bar{p}_{ij} - p_j > 0. \text{ In case of general impossibility of the phase transformation, we set } \bar{p}_{ij} = 0.$$

$$(2.39) \quad \text{For each phase } j \text{ there exist two temperatures } \theta_{jf} \text{ and } \theta_{js} \text{ generally depending on } \mathbf{u}_c \text{ such that the transformation } i \rightarrow j \text{ may only occur, if } \theta_{jf} \leq \theta < \theta_{js}. \text{ This last condition can be taken into account by a switch-off function } G_{ij}, \text{ which is equal to one, if the condition is fulfilled, and which is equal to zero otherwise.}$$

REMARK 2. Sometimes, the value \bar{p}_{ij} can be regarded as “equilibrium fraction” \bar{p}_i of the i -th phase (cf. [29, 30]). The approach here is more general, and we avoid the discussion about the precise notion of an equilibrium. Additionally, the controlling condition in (2.38) is more general as in [29, 30].

As usual, we define the Heaviside-function H by

$$(2.40) \quad H(s) := 0 \quad \text{when } s \leq 0, \quad H(s) = 1 \quad \text{when } s > 0.$$

Taking the assumptions (2.34), (2.35), (2.38) and (2.39) into account, we propose the subsequent general model for PT in steel

$$(2.41) \quad p'_i = - \sum_{j=1}^N a_{ij} H(p_i) H(\bar{p}_{ij} - p_j) G_{ij} + \sum_{j=1}^N a_{ji} H(p_j) H(\bar{p}_{ij} - p_i) G_{ji},$$

$$i = 1, \dots, N.$$

In this work, we deal with an unalloyed hypoeutectoid steel. Thus, the occurring phases are numbered as follows:

Table 1. Occurring phases in our situation of an unalloyed hypoeutectoid steel.

index	1	2	3	4	5
phase	austenite	ferrite	pearlite	bainite	martensite

Pre-eutectoid ferrite will also be denoted by the index 2. Based on the above, we write the following differential equations for the possible phase transformations *in our situation*:

$$(2.42) \quad p_1' = - \sum_{j=2}^5 a_{1j} H(p_1) H(\bar{p}_{1j} - p_j) G_{1j} + a_{21} H(p_2) H(\bar{p}_{21} - p_1) G_{21},$$

$$(2.43) \quad p_2' = a_{12} H(p_1) H(\bar{p}_{12} - p_2) G_{12} - a_{21} H(p_2) H(\bar{p}_{21} - p_1) G_{21},$$

$$(2.44) \quad p_i' = a_{1i} H(p_1) H(\bar{p}_{1i} - p_i) G_{1i}, \quad i = 3, 4, 5.$$

The switch-off functions G_{ij} are defined below as characteristic functions of specific regions in the iron-carbon diagram (cf. [7, 8, 22, 28, 33, 36], e.g.). By the Heaviside functions in (2.42) – (2.44), condition (2.38) is taken into account. Equation (2.42) describes the transformation of austenite into the ferritic phases as well as the inverse transformation of ferrite into austenite. Equation (2.43) describes the forming and depletion of ferrite, while (2.44) describes the forming of the remaining ferritic phases from austenite. The a_{ij} are modelled according to the concrete situation. Possible choices are the approaches by Johnson–Mehl–Avrami for diffusion-controlled transformations or that of Koistinen–Marburger for martensitic transformations). We make a general approach (see [20, 21, 49] for detailed discussions and also Remark 3):

$$(2.45) \quad a_{ij} := (e_{ij}(\theta, \mathbf{u}_c) + p_j)^{r_{ij}(\theta, \mathbf{u}_c)} (\bar{p}_j - p_j)^{s_{ij}(\theta, \mathbf{u}_c)} g_{ij}(\theta, \mathbf{u}_c),$$

The parameters e_{ij} , r_{ij} , s_{ij} and g_{ij} are subject to the conditions:

$$(2.46) \quad e_{ij} \geq 0, \quad r_{ij} \geq 0, \quad s_{ij} \geq 1, \quad g_{ij} \geq 0 \quad \text{for all admissible arguments.}$$

Therefore, for each transformation $i \rightarrow j$ ($i \neq j$), no more than four parameters have to be determined, either from dilatometer experiments for different relevant situations or from particular transformation diagrams (cf. [20, 49]). We will return to this in Sec. 4.2. We remark that there also exist approaches that account for an explicit dependence on the change in temperature θ' by an additional parameter (cf. [9, 10, 23]). In the present work, such a dependence is omitted. According to (2.32) it suffices to take only $N - 1$ ($= 4$) differential equations into account. We will therefore consider only (2.43) and (2.44) below. In our situation, specified by assumption 2 in 2.1, we add the following initial conditions:

$$(2.47) \quad p_1(x, 0) = 1, \quad p_j(x, 0) = 0 \quad \text{for } j = 2, \dots, N.$$

In Sec. 4.2 concrete descriptions for the bainitic and martensitic transformations are given.

REMARK 3. Well-known models for phase transformations in steel are included by the approach presented above. The linear model suggested by LEBLOND and DEVAUX [29, 30] reads for the formation of phase j from phase i (under conditions (2.38), (2.39))

$$(2.48) \quad p'_j = \frac{\bar{p}_i - p_i}{\tau_{ij}},$$

where τ_{ij} is a non-negative parameter having the dimension of time and characterising the transformation. This law is obtained by setting in the Eqs. (2.42)–(2.44)

$$(2.49) \quad a_{ij} := \tau_{ij}^{-1}.$$

The well-known model by Johnson, Mehl, Avrami and Kolmogoroff for diffusion-controlled transformations (see [9, 11, 12, 29, 30, 31], e.g.) reads for the formation of phase j from phase i (at constant temperature and under conditions (2.38), (2.39))

$$(2.50) \quad p_j(t) = \bar{p}_j \left(1 - \exp \left(- \left(\frac{t}{\tau_{ij}(\theta)} \right)^{n_{ij}(\theta)} \right) \right),$$

where $\tau_{ij} > 0$ and $n_{ij} > 1$ are parameters depending on temperature. From (2.50), follows in case of constant θ the differential equation

$$(2.51) \quad p'_j(t) = (\bar{p}_j - p_j(t)) \frac{n_{ij}(\theta)}{\tau_{ij}(\theta)} \left(-\ln(1 - p_j(t)\bar{p}_j^{-1}) \right)^{1 - \frac{1}{n_{ij}(\theta)}}.$$

Application of this equation for non-isothermal transformations is often inaccurate. Therefore, various modifications have been suggested (see [9, 10, 23, 29, 30, 37, 50], e.g.). We also note that the right-hand side of (2.51) does *not* have the structure of (2.45). However, this structure is obtained by linearising the logarithm in (2.51) in accordance with $-\ln(1 - x) \approx x$ for small x :

$$(2.52) \quad p'_j(t) = (\bar{p}_j - p_j(t)) \frac{n_{ij}(\theta)}{\tau_{ij}(\theta)} \left(p_j(t)\bar{p}_j^{-1} \right)^{1 - \frac{1}{n_{ij}(\theta)}}.$$

3. Phase transformations in an unalloyed hypoeutectoid steel

3.1. Determination of domains for the (macroscopic) carbon concentration and for the temperature

Now we describe the specific phase transformations occurring during quenching. In order to limit the modelling effort, we restrict to hypoeutectoid unalloyed

steel and we assume for the total mass fraction of carbon and for the temperature:

$$(3.1) \quad 0.0025 \leq u \leq 0.0083,$$

$$(3.2) \quad -100 \leq \theta \leq 1300.$$

The temperature is measured in $^{\circ}\text{C}$. For simplicity, we omit this unit in the equations. Thus, we consider (solid) steel being completely in the austenitic phase at equilibrium (with $u_{c1} = u$) at a temperature above 900°C (with u and θ subject to (3.1), (3.2)). Conditions (3.1), (3.2) define the section from the iron-carbon diagram in Fig. 1 relevant for our situation (cf. [7, 8, 22, 33, 36], e.g.). The lower bound for the temperature range (-100°C) is chosen rather arbitrarily, however, it allows for a low quenching temperature. For low-alloyed steel, one needs to take discrepancies in the iron-carbon diagram into account (see [7, 8, 22, 33, 36], e.g., and citations therein). The initial conditions (2.19), (2.30) are assumed to be compatible with (3.1) and (3.2). While in materials

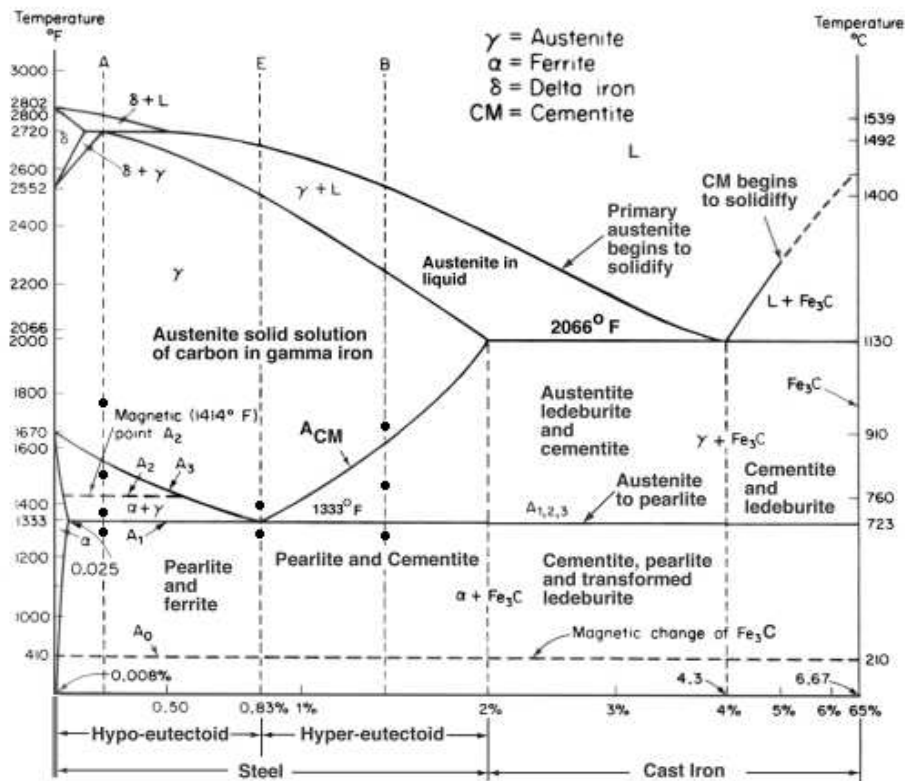


FIG. 1. Fe-Fe₃C phase diagram (taken from [36]).

science often the mass percentages are employed, we use mass fractions in the following equations, for consistency with the a.m.

We introduce the following curves in the iron-carbon diagram as graphs of functions depending on the carbon content u :

$$(3.3) \quad \text{curve GP:} \quad \theta = f_{GP}(u) \quad \text{for } 0 \leq u \leq 0.00025;$$

$$(3.4) \quad \text{curve GS:} \quad \theta = f_{GS}(u) \quad \text{for } 0 \leq u \leq 0.0083;$$

$$(3.5) \quad \text{curve SE:} \quad \theta = f_{SE}(u) \quad \text{for } 0.0083 \leq u \leq 0.0206;$$

$$(3.6) \quad \text{curve QP:} \quad \theta = f_{QP}(u) \quad \text{for } 0 \leq u \leq 0.00025.$$

We denote by f_{SE} the curve (dashed in Fig. 2) that is extended below 723°C for thermodynamic reasons. It represents the limit value for cementite (in pearlite). ($f_{SE}^1(\theta)$ is the minimum C concentration in austenite at which cementite can still be formed (as a constituent of pearlite)).

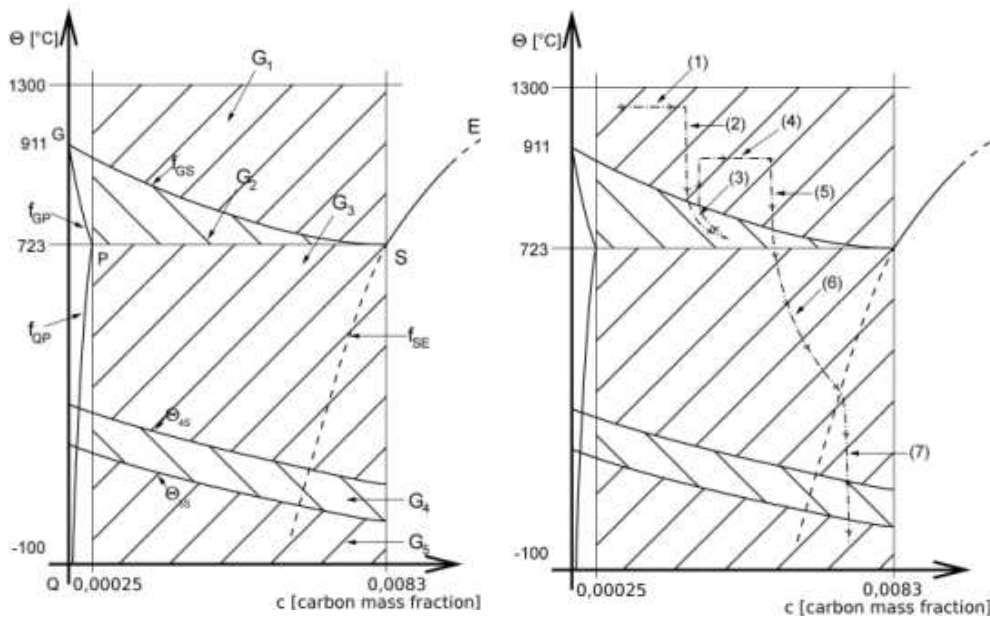


FIG. 2. Admissible carbon-temperature domains for the model under consideration (left), and a possible path of temperature and carbon mass fraction in austenite (right, see text).

The occurring phases are numbered in accordance with Table 1. Since only austenite is present at the beginning, we assume further

$$(3.7) \quad \theta_0(x) \geq f_{GS}(u_{c10}(x)) \quad \text{for } x \in \Omega.$$

Motivated by the Fe-Fe₃C diagram (Fig. 1), we define regions for temperature and carbon content, which split the range given in (3.1), (3.2) into disjoint parts (see Fig. 2):

$$(3.8) \quad G_1 \quad : \quad 0.00025 \leq u \leq 0.0083, \quad f_{GS}(u) < \theta \leq 1300;$$

$$(3.9) \quad G_2 \quad : \quad 0.00025 \leq u \leq 0.0083, \quad 723 < \theta \leq f_{GS}(u);$$

$$(3.10) \quad G_3 \quad : \quad \theta_{4s}(u) < \theta \leq 723 \quad 0.00025 \leq u \leq 0.0083;$$

$$(3.11) \quad G_4 \quad : \quad \theta_{5s}(u) < \theta \leq \theta_{4s}(u) \quad 0.00025 \leq u \leq 0.0083;$$

$$(3.12) \quad G_5 \quad : \quad -100 \leq \theta \leq \theta_{5s}(u) \quad 0.00025 \leq u \leq 0.0083.$$

Here the curves θ_{4s} and θ_{5s} represent the bainite and martensite start temperature. For unalloyed steel the martensite start temperature is a monotonically decreasing function w.r.t. carbon content in austenite. For the modelling, this monotonicity is not of importance. Corresponding to the domains G_i , we define characteristic functions via

$$(3.13) \quad \chi_{G_i}(u, \theta) := 1, \quad \text{if } (u, \theta) \in G_j, \quad \chi_{G_i}(u, \theta) := 0 \quad \text{otherwise} \\ \text{for } j = 1, \dots, 5.$$

The left-hand side of Fig. 2 shows the admissible domains. In the right-hand figure, a path is plotted which represents the possible evolution of carbon content in austenite and of temperature during carburisation and quenching, at a fixed position inside. At constant temperature, the pure austenite has a growing carbon content due to diffusion (carburisation) (part (1) in Fig. 2 (right)). After that, during cooling down, in G_1 , there is some small growth due to diffusion. Further on, in G_2 , due to the forming ferrite, the carbon content in austenite grows (part (2)). Contrary to that, a re-heating reduces the carbon content in austenite, but the diffusion shifts the part (3) to the right. Part (4) describes further carburisation at constant temperature. Finally, during cooling down, at first the carbon content in austenite remains almost constant (part (5)), followed by a growth due to ferrite formation (part (6)). Pearlite, bainite and martensite are formed without changing the carbon content in austenite (part (7)).

3.2. Special assumptions concerning the occurring phase transformations

We need some more assumptions, in addition to the general ones given in Sec. 2.1, describing the specific development of the possible phase transformations. Based on the iron-carbon diagram and the restriction given by (3.1), (3.2), we formulate assumptions which are suitable for practical use.

1. In the region G_1 only austenite is present (after sufficiently long time). According to (3.7), the process starts in this region.

2. In the region G_2 ferrite is formed. After sufficiently long time, we get an equilibrium between austenite and ferrite. A re-entry of θ and u from G_2 into G_1 is *allowed* (see Fig. 3).
3. In the region G_3 pre-eutectoid ferrite and pearlite can be formed. A transition from G_3 to G_2 (i.e. a re-heating above 723°C) is excluded.
4. If θ and u_{c1} reach values in G_4 , bainite is formed with the carbon content u_{c1} . A re-entry of θ and u_{c1} from G_4 into G_3 is *not* allowed.
5. If θ and u_{c1} reach values in G_5 , martensite is formed with the carbon content u_{c1} . A re-entry of θ and u_{c1} from G_5 into G_4 is allowed.
6. It is assumed that (local) diffusion of carbon in ferrite is sufficiently fast such that the carbon content in ferrite is always constant in space. In this way, we avoid the modelling of coexisting ferrite with different carbon content at different positions inside the sample. This assumption is motivated by the following facts: On the one hand, diffusion of carbon in ferrite is faster than in austenite (cf. [7, 8, 11, 33], e.g.); on the other hand, the carbon content in ferrite is small and does not change considerably (see iron-carbon diagram).

The last statement in assumption 3 is in accordance with assumption 2 in 2.1, which excludes a reverse transformation from pearlite, bainite and martensite to austenite. In contrast to the model in [47], we allow a transition from G_2 to G_1 . In doing so, we allow for a more general carbon temperature course during carburisation (cf. Fig. 2 (right), see [27], e.g.). When the temperature has dropped below the eutectoid temperature (723°C), it is not allowed to cross this value again, according to assumption 3. We have assumed the restriction in assumptions 4 for the sake of clarity. Otherwise, the model for forming ferrite and pearlite would be more complex.

3.3. Transformations between austenite and ferrite in the region G_2

As it can be read off the iron-carbon diagram, for each u (total carbon content) and each θ in G_2 , there exists an equilibrium fraction of ferrite $\bar{p}_{12}(u, \theta)$ with carbon content $f_{GP}^{-1}(\theta)$ and an equilibrium fraction of austenite $\bar{p}_{21}(u, \theta)$ with carbon content $f_{GS}^{-1}(\theta)$. From the mass balance of carbon (“lever rule”, see [7, 8], e.g.) it follows

$$(3.14) \quad u = f_{GS}^{-1}(\theta)\bar{p}_{21}(u, \theta) + f_{GP}^{-1}(\theta)\bar{p}_{12}(u, \theta)$$

if only austenite and ferrite are present. The quantities θ, u, u_{c1} , etc. depend on x and t , which we do not indicate explicitly. Using

$$(3.15) \quad \bar{p}_{21}(\theta, u) = 1 - \bar{p}_{12}(\theta, u) \quad \text{for } (u, \theta) \in G_2,$$

Eq. (3.14) gives

$$(3.16) \quad \bar{p}_{12}(u, \theta) = \frac{f_{GS}^{-1}(\theta) - u}{f_{GS}^{-1}(\theta) - f_{GP}^{-1}(\theta)} \quad \text{for } (u, \theta) \in G_2$$

with

$$(3.17) \quad u = u_{c1}p_1 + u_{c2}p_2.$$

In the region G_1 it holds, of course,

$$(3.18) \quad \bar{p}_{12}(u, \theta) = 0, \quad \bar{p}_{21}(\theta, u) = 1 \quad \text{for } (u, \theta) \in G_1.$$

We obtain the following differential equation for the transformation of austenite into ferrite (and vice versa) (cf. (2.43))

$$(3.19) \quad p_2' = \{a_{12}H(p_1)H(\bar{p}_{12}(u, \theta) - p_2) - a_{21}H(p_2)H(\bar{p}_{21} - p_1)\} \\ \times (\chi_{G_1}(u, \theta) + \chi_{G_2}(u, \theta)),$$

where a_{12} and a_{21} are both greater or equal to zero (cf. (2.37) and (2.45)). Due to (3.18), ferrite can be formed only in G_2 , while austenite in G_1 and G_2 . In accordance with assumption 6, from 3.2 we set

$$(3.20) \quad u_{c2}(x, t) = \varphi(\theta(x, t))$$

with φ defined (for further use) by

$$(3.21) \quad \varphi(\theta) := f_{GP}^{-1}(\theta)H(\theta - 723) + f_{QP}^{-1}(\theta)H(723 - \theta).$$

REMARK 4. The description of the carbon content in ferrite becomes more complicated without assumption 6 in 3.2. We refer to [47] for discussion.

3.4. Transformation of austenite into ferrite and pearlite in G_3

In G_3 , (pre-eutectoid) ferrite and pearlite can be formed. Generally, the transformation starts with the former, enlarging the carbon content in the remaining austenite. If this carbon content reaches the value $f_{SE}^{-1}(\theta)$, the remaining austenite will be transformed into pearlite (cf. [7, 8, 22]). In [47], we have used this approach of consecutive transformations. However, there is a disadvantage, when extracting the needed data only from the transformation diagrams. These diagrams represent an assumed simultaneous transformation (see Sec. 5). Thus, here we deal with this “simultaneous approach”. Due to the restriction in assumption 4 in 3.3, in G_3 only austenite, ferrite and pearlite are present. So we have (cf. (3.17), (3.20), (3.21))

$$(3.22) \quad u = u_{c1}p_1 + \varphi(\theta)p_2 + f_{SE}^{-1}(\theta)p_3 \quad \text{for } \theta_{4s}(u) < \theta \leq 723.$$

REMARK 5. Analogously to ferrite, we approximately assume that all existing pearlite has the carbon content $f_{SE}^{-1}(\theta)$. This is a compromise which has been found in the case of the assumed simultaneous transformations of pre-eutectoid ferrite and pearlite. We will return to this problem in Remark 6.

The equilibrium values for ferrite and pearlite are given by the lever rule again:

$$(3.23) \quad u = \varphi(\theta)\bar{p}_{12} + f_{SE}^{-1}(\theta)\bar{p}_{13}.$$

This leads to (cf. (3.15), (3.16), (3.22))

$$(3.24) \quad \bar{p}_{12}(u, \theta) = \frac{f_{SE}^{-1} - u}{f_{SE}^{-1}(\theta) - f_{QP}^{-1}(\theta)} \quad \text{for } (u, \theta) \in G_3,$$

$$(3.25) \quad \bar{p}_{13}(\theta, u) = 1 - \bar{p}_{12}(\theta u), \quad \text{for } (u, \theta) \in G_3.$$

Therefore we obtain the following differential equation for the formation of ferrite and pearlite (cf. (3.19))

$$(3.26) \quad p_2' = a_{12}H(p_1)H(\bar{p}_{12}(u, \theta) - p_2)\chi_{G_3}(u, \theta),$$

$$(3.27) \quad p_3' = a_{13}H(\bar{p}_{13}(u, \theta) - p_3)H(p_1)\chi_{G_3}(u, \theta).$$

where the functions a_{12} and a_{13} have to be determined (see Sec. 5).

3.5. Transformation of austenite into bainite and into martensite

Bainite can only be formed if $(u_{c1}, \theta) \in G_4$. Its carbon content is

$$(3.28) \quad u_{c4} = u_{c1}.$$

The possible final value (\bar{p}_{14}) is (cf. assumption 5 in 3.2)

$$(3.29) \quad \bar{p}_{14} = 1 - p_2 - p_3 - p_5.$$

The transformation equation for bainite reads then

$$(3.30) \quad p_4' = a_{14}H(\bar{p}_{14} - p_4)H(p_1)\chi_{G_4}(u_{c1}, \theta).$$

The formation of martensite is only possible if $(u_{c1}, \theta) \in G_5$. Clearly, it holds

$$(3.31) \quad u_{c5} = u_{c1}.$$

The still available austenite can be transformed into martensite by

$$(3.32) \quad p'_5 = a_{15}H(\bar{p}_5 - p_5)H(p_1)\chi_{G5}(u_{c1}, \theta).$$

The final value \bar{p}_{15} can be determined by the Koistinen-Marburger approach (see [6, 8, 9, 21, 29], e.g.) as

$$(3.33) \quad \bar{p}_{15} = (1 - p_2 - p_3 - p_4) \left(1 - \exp \left(-\frac{\theta_{5s}(u_{c1}) - \theta}{\theta_{m0}(u_{c1})} \right) \right).$$

Here, θ_{m0} is a parameter depending on the carbon concentration in austenite (see Sec. 5).

4. Bulk model of complex material behaviour

4.1. The general case

We summarise the mathematical model for our situation, which is described by the assumptions given in 3.2. Taking (2.32), (3.28) and (3.31) into account, the diffusion equation (2.16) reads as

$$(4.1) \quad \begin{aligned} \frac{\partial}{\partial t} \left((1 - p_2 - p_3)u_{c1} \right) - \operatorname{div} \left(d_{c1}(\theta)p_1 \nabla u_{c1} \right) \\ = -\frac{\partial}{\partial t} \left(u_{c2}p_2 \right) - \frac{\partial}{\partial t} \left(u_{c3}p_3 \right) \quad \text{in } \Omega \times]0, T[. \end{aligned}$$

From (2.27) we obtain the heat equation, in our setting:

$$(4.2) \quad \begin{aligned} \rho c_e \theta' - \operatorname{div} (\kappa(\mathbf{u}_c, \theta, \mathbf{p}) \nabla \theta) = \rho L_2(u_{c1}p_1 + u_{c2}p_2, \theta)p'_2 \\ + \rho L_2(u_{c1}, \theta)p'_3 + \rho L_4(u_{c1}, \theta)p'_4 + \rho L_5(u_{c1}, \theta)p'_5 \quad \text{in } \Omega \times]0, T[. \end{aligned}$$

The latent heat of the transformations between austenite and ferrite depends on the carbon content of the mixture of austenite and ferrite, whereas the latent heats of the remaining transformations depend on the carbon content in austenite. Due to (3.19), (3.26), (3.27), (3.30), (3.32), the transformation equations for ferrite, pearlite, bainite and martensite read as

$$(4.3) \quad \begin{aligned} p'_2 = \left\{ a_{12}H(p_1)H(\bar{p}_{12}(u, \theta) - p_2) - a_{21}H(p_2)H(\bar{p}_{21} - p_1) \right\} \\ \times \left(\chi_{G1}(u, \theta) + \chi_{G2}(u, \theta) \right) + a_{12}H(p_1)H(\bar{p}_{12}(u, \theta) - p_2)\chi_{G3}(u, \theta) \\ \text{in } \Omega \times]0, T[, \end{aligned}$$

$$(4.4) \quad p'_3 = a_{13}H(\bar{p}_{13} - p_3)H(p_1)\chi_{G3}(u, \theta) \quad \text{in } \Omega \times]0, T[,$$

$$(4.5) \quad p'_4 = a_{14}H(\bar{p}_{14} - p_4)H(p_1)\chi_{G4}(u_{c1}, \theta) \quad \text{in } \Omega \times]0, T[,$$

$$(4.6) \quad p'_5 = a_{15}H(\bar{p}_{15} - p_5)H(p_1)\chi_{G5}(u_{c1}, \theta) \quad \text{in } \Omega \times]0, T[,$$

where the maximum values of the phase fractions of austenite, ferrite, pearlite and bainite are given as follows (cf. (3.16), (3.18), (3.24), (3.25), (3.29), (3.33)):

$$(4.7) \quad \bar{p}_{12}(u, \theta) = 0 \quad \text{for } (u, \theta) \in G_1,$$

$$(4.8) \quad \bar{p}_{12}(u, \theta) = \frac{f_{GS}^{-1}(\theta) - u_{c1} p_1 - u_{c2} p_2}{f_{GS}^{-1}(\theta) - f_{GP}^{-1}(\theta)} \quad \text{for } (u, \theta) \in G_2,$$

$$(4.9) \quad \bar{p}_{12}(u, \theta) = \frac{f_{SE}^{-1}(\theta) - u_{c1} p_1 - u_{c2} p_2 - u_{c3} p_3}{f_{SE}^{-1}(\theta) - f_{QP}^{-1}(\theta)} \quad \text{for } (u, \theta) \in G_3,$$

$$(4.10) \quad \bar{p}_{13}(\theta, u) = 1 - \bar{p}_{12}(\theta, u) \quad \text{for } (u, \theta) \in G_3,$$

$$(4.11) \quad \bar{p}_{14} = 1 - p_2 - p_3 - p_5,$$

$$(4.12) \quad \bar{p}_{15} = (1 - p_2 - p_3 - p_4) \left(1 - \exp \left(-\frac{\theta_{5s}(u_{c1}) - \theta}{\theta_{m0}(u_{c1})} \right) \right).$$

Moreover, the quantity u_{c2} and u_{c3} are given by (cf. Remarks 4 and 5)

$$(4.13) \quad u_{c2} = \varphi(\theta), \quad u_{c3} = f_{SE}^{-1}(\theta),$$

and φ is defined by (3.21).

REMARK 6. In our model, pre-eutectoid ferrite and pearlite are formed simultaneously (in G_3). But, actually, most of the pearlite is formed when the formation of ferrite is nearly finished, and u_{c1} has reached $f_{SE}^{-1}(\theta)$. Thus, it makes sense to change u_{c3} in the last term in (4.1) for u_{c1} . Therefore, under this assumption, instead of (4.1), we obtain the equation

$$(4.14) \quad \frac{\partial}{\partial t} \left((1 - p_2)u_{c1} \right) - \text{div} (d_{c1}(\theta)p_1 \nabla(u_{c1})) = -\frac{\partial}{\partial t} (u_{c2}p_2) \quad \text{in } \Omega \times]0, T[.$$

The initial conditions for u_{c1} , θ and p are

$$(4.15) \quad u_{c1}(x, 0) = u_{c10}(x), \quad \theta(x, 0) = \theta_0(x) \quad \text{for } x \in \Omega,$$

$$(4.16) \quad p_1(x, 0) = 1, \quad p_i(x, 0) = 0 \quad \text{for } i = 2, \dots, 5 \quad \text{for } x \in \Omega.$$

Moreover, the boundary conditions (2.18) (or, alternatively, (2.17)) for u and (2.27) for θ have to be added:

$$(4.17) \quad -d_{c1}(\theta) \frac{\partial}{\partial \mathbf{v}}(u_{c1}) = \delta_{c1}(\theta) \mu_c^0(\theta) \left(u_{c1} - \frac{c_c \Gamma}{\rho} \right) \quad \text{at } \partial\Omega \times]0, T[,$$

$$(4.18) \quad -\kappa \frac{\partial \theta}{\partial \mathbf{v}} = \delta_\theta(\theta - \theta_\Gamma) \quad \text{at } \partial\Omega \times]0, T[.$$

Here, θ_0 and u_{c10} have to satisfy condition (3.7).

Summing up, the mathematical model for the macroscopic modelling of carbon diffusion (in austenite), heat conduction and phase transformations, consists of an initial-boundary-value problem for a coupled system of two parabolic partial differential equations (4.1) (or, alternatively, (4.14)) and (4.2), and of several ordinary differential equations (4.3)–(4.6), in which the spatial variable x is a parameter. The equilibrium fractions of the phases (4.7)–(4.12) as well as (4.13) can be plugged into Eqs. (4.1)–(4.6) and can therefore be (formally) eliminated. Due to various nonlinearities, the mathematical and numerical investigations are *nontrivial*. A suitable solution theory for the bulk model would essentially exceed the scope of the present paper. This can be done basing on the concept of weak solutions (cf. [40, 51], e.g., for details and discussion). We refer to [25] for some mathematical results.

4.2. A special case – transformation of austenite only into bainite and martensite

The general mathematical model is rather complex. Therefore it has to be investigated which simplifications can be made. For instance, if the workpiece intended for case hardening is not too large, then it is reasonable to assume that austenite transforms *only* into bainite and martensite. As a special case of the problem described in 4.1, one obtains the following equations (where (4.19) is a special case of (4.1))

$$(4.19) \quad u'_{c1} - \operatorname{div}(d_{c1}(\theta) p_1 \nabla u_{c1}) = 0 \quad \text{in } \Omega \times]0, T[,$$

$$(4.20) \quad \begin{aligned} \rho_{c_e} \theta' - \operatorname{div}(\kappa(\mathbf{u}_c, \theta, \mathbf{p}) \nabla \theta) \\ = \rho L_4(u_{c1}) p'_4 + \rho L_5(u_{c1}) p'_5 \end{aligned} \quad \text{in } \Omega \times]0, T[,$$

$$(4.21) \quad p'_4 = a_{14} H(1 - p_5 - p_4) H(p_1) \chi_{G4}(u_{c1}, \theta) \quad \text{in } \Omega \times]0, T[,$$

$$(4.22) \quad p'_5 = a_{15} H(\bar{p}_{15} - p_5) H(p_1) \chi_{G5}(u_{c1}, \theta) \quad \text{in } \Omega \times]0, T[,$$

$$(4.23) \quad \bar{p}_{15} = (1 - p_4) \left(1 - \exp \left(- \frac{\theta_{5s}(u_{c1}) - \theta}{\theta_{m0}(u_{c1})} \right) \right) \quad \text{in } \Omega \times]0, T[,$$

$$(4.24) \quad p_1 = 1 - p_4 - p_5 \quad \text{in } \Omega \times]0, T[.$$

The initial and boundary conditions have to be chosen as in 4.1.

4.3. Separation of diffusion and phase transformations

A second essential simplification can be made by considering the different time scales at which diffusion and phase transformations take place (during quenching). If carbon diffusion happens only in region G_1 , then (in G_1) diffusion and heat conduction can be described by two coupled parabolic partial differential equations without sources:

$$(4.25) \quad u'_{c1} - \operatorname{div}(d_{c1}(\theta)\nabla u_{c1}) = 0 \quad \text{in } \Omega \times]0, T[,$$

$$(4.26) \quad \rho_{ce}\theta' - \operatorname{div}(\kappa(\mathbf{u}_c, \theta)\nabla\theta) = 0 \quad \text{in } \Omega \times]0, T[.$$

(Of course p_1 is equal to one in G_1). Here we have to add the initial and boundary conditions (4.15), (4.17), (4.18) for u_{c1} and θ . The solution of (4.25), (4.26) gives the carbon distribution in the workpieces.

Assuming that quenching starts at time $t_1 > 0$, one can neglect macroscopic carbon diffusion after this moment. Hence, the second part of the problem consists in solving the coupled system of the heat equation and of the phase-transformation equations, using the already known $u_{c1} = u_{c1}(x, t_1)$.

Such a separation between diffusion during carburisation and subsequent quenching (with fixed carbon content) is also performed in commercial simulation software such as SYSWELD. We note that our model covers more complicated situations, when phase transformations (between austenite and ferrite, e.g.) take place during carburisation.

5. Numerical simulations

The bulk model summarised in 4.1 can be solved numerically, for instance, by the Finite-Element Method. In one space dimension, this can be established with relatively low effort using the MATLAB-routine `pdepe`. The system is first discretised in space, and the resulting system of ordinary differential equations is integrated by a solver that selects the time steps dynamically. Alternatively, it is possible to discretise the system, at first, in time (in an implicit or semi-implicit way). This allows for decoupling of the equations to be solved in each time step and is therefore expected to work more efficiently with the numerous nonlinearities in the model. This will become vitally important when doing simulations in

two or three space dimensions. An additional difficulty is given by the Heaviside and the characteristic functions occurring in the model. We approximate them by smooth functions.

Presenting some calculations, we show how the model developed above can be applied in concrete situations. The general problem consists in determining the material parameters. As we do not have complete experimental data, we act as follows: we withdraw the parameters concerning the phase transformation from TTT diagrams for two hypoeutectoid steels differing by carbon content. By interpolation between the corresponding values for “low” and “high” carbon content, we obtain the parameters as functions for arbitrary carbon content (between the boundary values). For the sake of simplicity, we use a given carbon content (cf. the discussion in Sec. 4.3). Therefore, one has a coupling of the heat-conduction equation and of the PT equations. From the TTT diagrams we obtain the coefficients τ and n for the Johnson–Mehl–Avrami approach (for forming of the ferrite, pearlite and bainite). The more general approach presented in Sec. 2.4 needs more experimental data. The martensitic transformation is modelled by the approach due to LEBLOND–DEVAUX [29, 30].

Thus, the coefficients a_{1j} ($j = 2, \dots, 5$) are (cf. (2.51))

$$(5.1) \quad a_{1j} := (\bar{p}_{1j}(u, \theta) - p_j(t)) \frac{n_{1i}}{\tau_{1j}} \left(-\ln(1 - p_j(t)\bar{p}_{1j}^{-1}) \right)^{1 - \frac{1}{n_{1j}(\theta)}}, \quad j = 2, 3, 4,$$

$$(5.2) \quad a_{15} = \bar{p}_{15}(u, \theta) - p_5(t) \mu_{15}.$$

Inserting (5.1) and (5.2) into (4.3) (only with respect to G_3), and into (4.4)–(4.6), we get the system describing the phase transformations:

$$(5.3) \quad p'_j = \max \left\{ \bar{p}_{1j}(u, \theta) - p_j, 0 \right\} \frac{n_{1i}}{\tau_{1j}} \cdot \left(-\ln(1 - p_j(t)\bar{p}_{1j}^{-1}) \right)^{1 - \frac{1}{n_{1j}(\theta)}} H(p_1) \chi_{G_3}(u, \theta) \quad \text{for } j = 2, 3,$$

$$(5.4) \quad p'_4 = \max \left\{ \bar{p}_{14}(u, \theta) - p_4, 0 \right\} \frac{n_{14}}{\tau_{14}} \cdot \left(-\ln(1 - p_4(t)\bar{p}_{14}^{-1}) \right)^{1 - \frac{1}{n_{14}(\theta)}} H(p_1) \chi_{G_4}(u, \theta),$$

$$(5.5) \quad p'_5 = \max \left\{ \bar{p}_{15} - p_5, 0 \right\} \mu_5 H(p_1) \chi_{G_5}(u, \theta).$$

The limit values are given by (4.9)–(4.12). In (5.1)–(5.5), u is the given (total) carbon concentration being equal to the initial value of u_{c1} . The switch-off function χ_{G_j} will be constructed in accordance with information from the TTT diagrams.

In order to obtain realistic data, we take TTT diagrams for the steels 1320 (carburised with 0.4% C – named as steel 0.4) and 1320 (carburised with 0.6% C – named as steel 0.6) from [42] (page 17). As usual in the TTT diagrams, the information about the transformation of austenite into ferrite and vice versa between austenite-start and final temperature (A_{c1} and A_{c3}) is incomplete. Hence, we neglect phase transformations above 730° C. The cited diagrams yield the subsequent information (cf. [25] for details).

For the domains of PT:

$$(5.6) \quad G_3 : 525^\circ\text{C} \leq \theta \leq 730^\circ\text{C} \quad \text{for both steels } 0.4 \text{ and } 0.6,$$

$$(5.7) \quad G_4 : 333^\circ\text{C} \leq \theta \leq 525^\circ\text{C} \quad \text{for the steel } 0.4,$$

$$G_4 : 256^\circ\text{C} \leq \theta \leq 525^\circ\text{C} \quad \text{for the steel } 0.6.$$

For steels with carbon content between 0.4% and 0.6% we obtain G_4 by linear interpolation. Hence, the martensite-start temperature is given by

$$(5.8) \quad \theta_{5s}(u) = 256 \frac{u - 0.004}{0.002} + 333 \frac{0.006 - u}{0.002} \text{ [}^\circ\text{C]} \\ \text{for } 0.004 \leq u \leq 0.006.$$

The Koistinen–Marburger parameter θ_{m0} (cf. (3.33)) can be obtained via the line indicating 90% of martensite forming. Thus, we have

$$(5.9) \quad \theta_{m0}(u) = 60.37 \frac{u - 0.004}{0.002} + 46.04 \frac{0.004 - u}{0.002} \text{ [}^\circ\text{C]} \\ \text{for } 0.004 \leq u \leq 0.006.$$

For the parameter μ_5 in (5.5), we take the value

$$(5.10) \quad \mu_5 = 50 \text{ [sec}^{-1}\text{]},$$

using a suggestion in [29]. (This information cannot be taken from the diagram).

The parameters n and τ for the JMAK approach in (5.3), (5.4) can be extracted from the diagrams, using the 1% and 99% curves for some discrete temperature values. For technical reasons, we limit the values for n by 1 from below (cf. (5.3), (5.4)). The parameters for the bainitic transformation are listed in the Tables 2 and 3:

Table 2. Parameter n_4 and τ_4 for the bainitic transformation for the steel 0.4.

θ [° C]	369	400	428	447	489
n_4	1.198	1.33	1.348	1.312	1.074
τ_4 [sec ⁻¹]	139.7	63.5	51.6	50.0	72.4

Table 3. Parameter n_4 and τ_4 for the bainitic transformation for the steel 0.6.

θ [° C]	314	350	389	425	483	500
n_4	1.567	1.459	1.331	1.320	1.223	1.200
τ_4 [sec ⁻¹]	1886	702.2	158.7	88.05	86.05	92.43

By linear interpolation, we obtain the parameters in Tables 1 and 2 as functions of θ , keeping the outer values constant up to the boundary of the existence interval of bainite. After this, interpolating over the carbon content, we have

$$(5.11) \quad n_4(\theta, u) = n_{4,0.6}(\theta) \frac{u - 0.004}{0.002} + n_{4,0.4}(\theta) \frac{0.006 - u}{0.002}$$

for $0.004 \leq u \leq 0.006$,

and, analogously, for τ_4 . For the transformation into pre-eutectoid ferrite and pearlite one needs the values of the functions f_{QP} and f_{SE} (cf. Fig. 2, left). These values have been provided from the Institut für Werkstofftechnik Bremen (IWT). Hence, one can calculate the equilibrium values \bar{p}_{12} , \bar{p}_{13} by formulas (4.9) and (4.10). Using the diagrams again, we obtain the parameters n and τ for the transformations into ferrite and pearlite. (In this area, the middle curve is regarded as the 99% curve of \bar{p}_{12} as well as the 1% curve of pearlite, (cf. [25, 50] for details). The parameters are listed in the Tables 4 and 5.

Table 4. Parameter n_2 , n_3 , τ_2 and τ_3 for the transformation into ferrite and pearlite for the steel 0.4.

θ [° C]	567	592	622	650	661
n_2	4.981	1.742	1.0	1.0	1.0
τ_2 [sec ⁻¹]	2.267	14.03	384.7	12310	8802
n_3	1.0	1.078	1.610	1.439	1.0
τ_3 [sec ⁻¹]	1244	712.3	3482	122315	1015652

Again, we obtain functions depending on θ , and u (cf. (5.11)). The remaining values needed for calculations are the parameters of heat conduction.

We simulate spatially one-dimensional problems which can model the evolution of phases and temperature over the depth of a workpiece. At one end of the interval (the assumed quenching side), we employ the boundary condition

Table 5. Parameter n_2 , n_3 , τ_2 and τ_3 for the transformation into ferrite and pearlite for the steel 0.6.

θ [° C]	569	606	622	644	661
n_2	4.730	2.267	1.658	1.296	1.028
τ_2 [sec ⁻¹]	7.935	45.67	144.2	696.6	4392
n_3	1.455	2.272	2.248	2.218	1.486
τ_3 [sec ⁻¹]	118.2	151.5	386.9	1591	22069

(4.18), while at the other end (inside the body), we assume thermal insulation (i.e. $\delta_\theta = 0$). We assume the depth of penetration of 50 mm. We consider alternatively two cooling situations:

- Quenching by gas nozzles with $\delta_\theta = 455 \left[\frac{\text{W}}{\text{m}^2\text{K}} \right]$;
- Quenching by water as during the Jominy test with $\delta_\theta = \delta_\theta(\theta)$ given in Fig. 3 (taken from [35]).

For the sake of simplicity, we chose for density and specific heat:

$$(5.12) \quad \rho = 7800 \left[\frac{\text{kg}}{\text{m}^3} \right], \quad c_e = 600 \left[\frac{\text{J}}{\text{kgK}} \right].$$

The heat conductivities and the latent heats are given in Fig. 3.

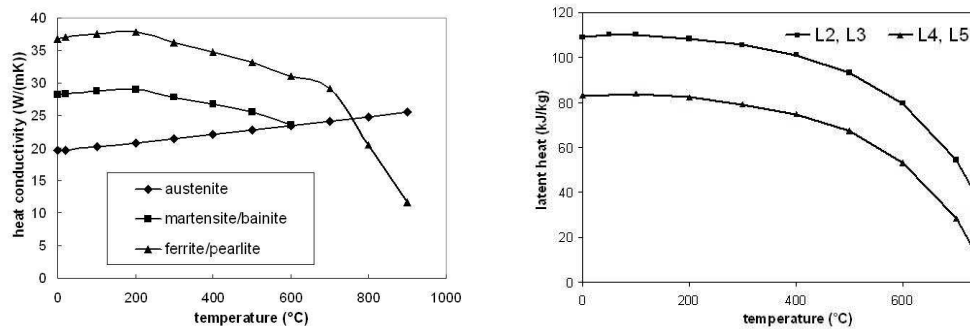


FIG. 3. Heat conductivities of the phases (left) and latent heats of the transformation of austenite into the ferritic phases (right) as functions of temperature.

We perform simulations for a constant carbon content of 0.4% as well as for a given carbon profile decreasing from 0.6% near the boundary to 0.4% in the middle of the body (see Fig. 4).

In Figs. 5 and 6, one can see the influence of carbon content and quenching regime on the final phase distribution over the depth of the workpiece. For instance, moderate quenching may lead to a nearly equal phase distribution over

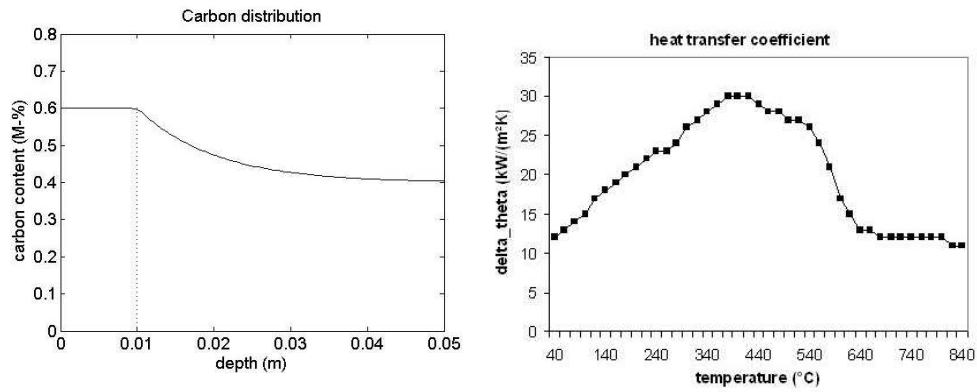


FIG. 4. Carbon profile over the depth (left) and heat-exchange coefficient for quenching during the Jominy test (right – cf. [35]).

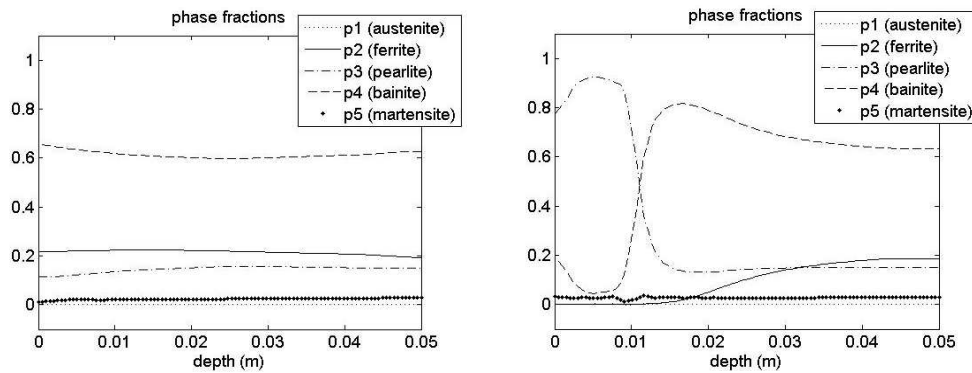


FIG. 5. Final phase distribution over the depth after quenching by gas nozzles ($\delta_\theta = 455$ [W/m² K] for 0.4% C (left) and for a carbon distribution as in Fig. 4 (right)).

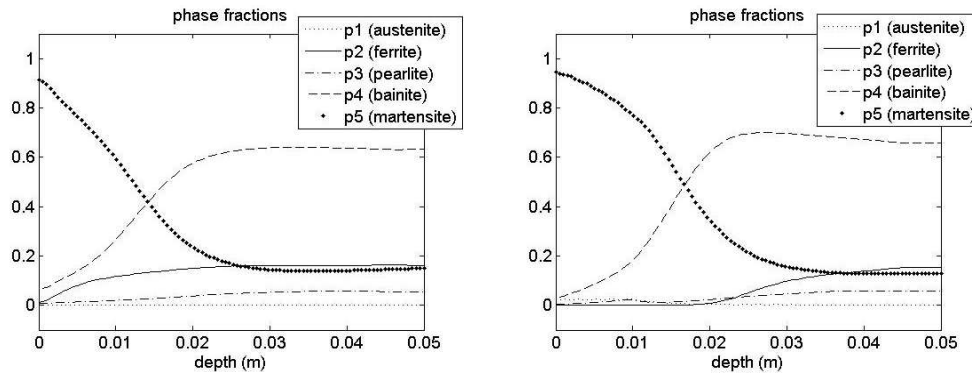


FIG. 6. Final phase distribution over the depth after quenching like during the Jominy test (see Fig. 4) for 0.4% C (left) and for a carbon distribution as in Fig. 4 (right).

the depth in the case of constant carbon content (Fig. 5, left), while the same quenching gives a qualitatively different result for the inhomogeneous carbon profile (Fig. 5, right). As expected, the very fast quenching as that during the Jominy test yields a large martensite fraction near the boundary (Fig. 6).

6. Summary and several remarks

We have modelled carbon diffusion, heat conduction and ferritic phase transformations in an unalloyed hypoeutectoid steel. The resulting mathematical model consists of a coupled system of two parabolic partial differential equations for carbon diffusion through the austenite and for heat conduction as well as ordinary differential equations for the evolution of the phase-fraction.

For a special case we have performed numerical simulations with realistic data. Hence, we have demonstrated how to apply the model developed for concrete situations. The results of the simulations describe the expected scenarios qualitatively correct.

We conclude with several remarks:

1. The model presented above can be extended via the “building-block principle”. Hence, it is possible to extend this model to a more general material behaviour (cf. [19, 32, 34] for basics, e.g.) of steel, taking mechanical movement into account (plasticity, transformation-induced plasticity, e.g.) (cf. [3, 13–15, 26, 31, 44–46, 48] for details and discussions concerning steel specifics). This work remains for future investigations.
2. The grain size of austenite plays an important role for the properties of the final workpiece. In [29], a differential equation for the average austenite grain size depending on temperature and phase evolution was proposed. In principle, one can add such an equation to the model of material behaviour (taking mechanical behaviour into account or not).
3. The hardness of the steel workpiece essentially depends on martensite fraction and on the carbon content (cf. [7, 8, 33, 36] e.g.). Using a formula describing the hardness as a function of martensite fraction and of carbon content, one can calculate *a posteriori* the hardness near the boundary.

Acknowledgments

This work has been partially supported by the German Research Foundation (DFG) with a grant through the Collaborative Research Centre SFB 570 „Distortion Engineering“ at the University of Bremen. The material data was partially provided by the Institut für Werkstofftechnik (IWT) Bremen. The authors thank Jochen Rath for preparing the figures and Isabel Hübler for assistance in preparing the numerical examples.

References

1. C. ACHT, B. CLAUSEN, F. HOFFMANN, H.-W. ZOCH, *Simulation of the distortion of 20MnCr5 parts after asymmetrical carburization*, Mat.-wiss. u. Werkstofftech., **37**, 152–156, 2006.
2. C. ACHT, T. LÜBBEN, F. HOFFMANN, H.-W. ZOCH, *Einfluss von Prozessparametern und Abmessungsvarianten auf die Maß- und Formänderung einsatzgehärteter Scheiben aus 20MnCr5*, HTM Z. Werkst. Waermebeh. Fertigung, **61**, 1, 3–42, 2006.
3. U. AHRENS, *Beanspruchungsabhängiges Umwandlungsverhalten und Umwandlungsplastizität niedrig legierter Stähle mit unterschiedlich hohen Kohlenstoffgehalten*, Diss., Universität Paderborn, Germany 2003.
4. H. ALDER, D. HÖMBERG, W. WEISS, *Simulationsbasierte Regelung der Laserhärtung von Stahl*, HTM Z. Werkst. Waermebeh. Fertigung, **61**, 2, 103–107, 2006.
5. H. ALTENA, F. SCHRANK, S. HEINECK, *Prozessüberwachung und Regelung von Niederdruckaufkohlungsprozessen*, HTM Z. Werkst. Waermebeh. Fertigung, **61**, 4, 195–205, 2006.
6. J. BEAR, Y. BACHMAT, *Introduction to modeling of transport phenomena in porous media*, Kluwer Academic, 1990.
7. H. BERNS, W. THEISEN, *Eisenwerkstoffe – Stahl und Gusseisen*, Springer-Verlag, Berlin 2006.
8. W. BLECK, *Werkstoffkunde Stahl für Studium und Praxis*, Verlag Mainz, Aachen 2001.
9. M. BÖHM, S. DACHKOVSKI, M. HUNKEL, T. LÜBBEN, M. WOLFF, *Übersicht über einige makroskopische Modelle für Phasenumwandlungen im Stahl*, Berichte aus der Technomathematik, FB 3, Universität Bremen, Report 03–09, <http://www.math.uni-bremen.de/zetem/>, 2003.
10. M. BÖHM, M. HUNKEL, A. SCHMIDT, M. WOLFF, *Evaluation of various phase-transition models for 100Cr6 for application in commercial FEM programs*, J. de Physique IV, **120**, 581–589, 2004.
11. J. BURKE, *The kinetics of phase transformations in metals*, Pergamon Press, Oxford 1965.
12. J. W. CHRISTIAN, *The theory of transformations in metals and alloys*, Part 1, Pergamon Press, Oxford 1975.
13. S. DENIS, P. ARCHAMBAULT, E. GAUTIER, A. SIMON, G. BECK, *Prediction of residual stress and distortion of ferrous and non-ferrous metals: current status and future developments*, J. of Materials Eng. and Performance, **11**, 1, 92–102, 2002.
14. M. DALGIC, G. LÖWISCH, *Einfluss einer aufgeprägten Spannung auf die isotherme, perlitische und bainitische Umwandlung des Wälzlagerstahls 100Cr6*, HTM Z. Werkst. Waermebeh. Fertigung, **59**, 1, 28–34, 2004.
15. F. D. FISCHER, [in:] *Modelling and simulation of transformation induced plasticity in elasto-plastic materials*, *Mechanics of solids with phase changes*, no. 368, M. BERGVEILLER, F. D. FISCHER [Eds.], Springer-Verlag, 1997.
16. R. FORTUNIER, J.B. LEBLOND, J.M. BERGHEAU, *A numerical model for multiple phase transformations in steels during thermal processes*, J. Shanghai Jiaotong Un., E5, No 1, 213, 2000.
17. J. GRUNEWALD, *Diffusiver und konvektiver Stoff- und Energietransport in kapillarporösen Baustoffen*, Diss., Technische Universität Dresden, Germany 1997.
18. A. G. GUY, *Metallkunde für Ingenieure*, Akad. Verlagsgesellschaft, Frankfurt 1983.

19. P. HAUPT, *Continuum Mechanics and Theory of Materials*, Springer-Verlag, Berlin 2000.
20. D. HÖMBERG, W. WEISS, *PID control of laser surface hardening of steel*, IEEE Transactions on Control Systems Technology, **14**, 5, 896904, 2006.
21. D. HÖMBERG, A. KHLUDNEV, *A thermoelastic contact problem with a phase transition*, IMA Journal of Applied Mathematics **71**, 4, 479–495, 2006.
22. D. HORSTMANN, *Das Zustandsschaubild Eisen-Kohlenstoff und die Grundlagen der Wärmebehandlung der Eisen-Kohlenstoff-Legierungen*, 5-th edition, Verlag Stahleisen, Düsseldorf 1992.
23. M. HUNKEL, T. LÜBBEN, F. HOFFMANN, P. MAYR, *Modellierung der bainitischen und perlitischen Umwandlung bei Stählen*, Haertereitechn. Mitt., **54**, 6, 365–372, 1999.
24. K. HUTTER, K. JÖHNK, *Continuum methods of physical modeling*, Springer, Berlin, Heidelberg 2004.
25. I. HÜSSLER, *Mathematische Untersuchungen eines gekoppelten Systems von ODE und PDE zur Modellierung von Phasenumwandlungen im Stahl*, Diploma thesis, Universität Bremen, FB 3, April 2007.
26. T. INOUE, Z. WANG, K. MIYAO, *Quenching stress of carburized steel gear wheel*, ICRS2, G. BECK, S. DENIS, A. SIMON [Eds.], Elsevier Appl. Sci., London, New York, 606–611, 1989.
27. J. KLEFF, S. HOCK, I. KELLERMANN, M. FLEISCHMANN, A. KÜPER, *Hochtemperatur-Aufkohlen – Einflüsse auf das Verzugverhalten schwerer Getriebebauteile*, HTM Z. Werkst. Waermebeh. Fertigung, **60**, 6, 311–316, 2005.
28. D. KOHTZ, *Wärmebehandlung metallischer Werkstoffe*, VDI, Düsseldorf 1994.
29. J. B. LEBLOND, J. DEVAUX, *A new kinetic model for anisothermal metallurgical transformations in steels including effect of austenite grain size*, Acta Met., **32**, 137–146, 1984.
30. J. B. LEBLOND, G. MOTTET, J. DEVAUX, J.C. DEVAUX, *Mathematical models of anisothermal phase transformations in steels, and predicted plastic behaviour*, Materials Science and Technology, **1**, 815–822, 1985.
31. J. LEMAITRE, *Handbook of Materials Behavior Models*, Academic Press, San Diego, USA 2001.
32. J. LEMAITRE, J.-L. CHABOCHE, *Mechanics of solid materials*, Cambridge University Press, Cambridge 1990.
33. W. C. LESLIE, *The physical metallurgy of steels*, McGraw-Hill, New York 1981.
34. I. MÜLLER, *Thermodynamik – Grundlagen der Materialtheorie*, Bertelsmann Universitätsverlag, Düsseldorf 1973.
35. M. NARAZAKI, M. KOGAWARA, A. SHIRAYORI, S. FUCHIZAWA, *Validation of material property data for quenching simulation by end-quench test and its simulation*, Proc. 1st Int. Conf. on Distortion Engineering, 14–16.09.2005 in Bremen, Germany, ZOCH, H.-W. [Eds.], Lübben, Th., 307–314.
36. POLLACK, *Materials Science and Metallurgy*, 4-th ed., Prentice-Hall, 1988.
37. T. RÉTI, L. HORVÁTH, I. FELDE, *A comparative study of methods used for the prediction of nonisothermal austenite decomposition*, J. of Mat. Eng. and Performance, **6**, 4, 433–442, 1997.
38. T. RÉTI, Z. FRIED, I. FELDE, *Computer simulation of steel quenching process using a multi-phase transformation model*, Computational Material Science, **22**, 261–278, 2001.

39. A. SCHMIDT, B. SUHR, T. MOSHAGEN, M. WOFF, M. BOEHM, *Adaptive finite element simulations for macroscopic and mesoscopic models*, Mat.-wiss. u. Werkstofftech., **37**, 142–146, 2006.
40. R. E. SHOWALTER, *Monotone Operators in Banach Spaces and Nonlinear Partial Differential Equations*, American Mathematical Society, 1997.
41. M. STEINBACHER, B. CLAUSEN, F. HOFFMANN, P. MAYR, H.-W. ZOCH, *Thermogravimetrische Messungen zur Charakterisierung der Reaktionskinetik beim Niederdruckaufkohlen*, HTM Z. Werkst. Waermebeh. Fertigung, **61**, 4, 186–194, 2006.
42. G.F. VANDER VOORT, *Atlas of time-temperature diagrams for irons and steels*, ASM International, 1991.
43. M. WOLFF, M. BÖHM, S. DACHKOVSKI, *Volumenanteile versus Massenanteile – der Dilatometerversuch aus der Sicht der Kontinuumsmechanik*, Berichte aus der Technomathematik, FB 3, Universität Bremen, Report 03-01, <http://www.math.uni-bremen.de/zetem/>, 2003.
44. M. WOLFF, M. BÖHM, A. SCHMIDT, *A thermodynamically consistent model of the material behaviour of steel including phase transformations, classical and transformation-induced plasticity*, in Trends in Applications of Mathematics to Mechanics, Shaker Verlag, Aachen, 591–601, W. YONGQI, H. KOLUMBAN [Eds.], 2005.
45. M. WOLFF, M. BÖHM, A. SCHMIDT, *Modelling of steel phenomena and its interactions – an internal-variable approach*, Mat.-wiss. u. Werkstofftech., **37**, 147–151, 2006.
46. M. WOLFF, M. BÖHM, *Transformation-induced plasticity in steel – general modelling, analysis and parameter identification*, Berichte aus der Technomathematik, FB 3, Universität Bremen, Report 06-02, <http://www.math.uni-bremen.de/zetem/>, 2006.
47. M. WOLFF, M. BÖHM, S. MEIER, *Modellierung der Wechselwirkung von Kohlenstoff-Diffusion und ferritischen Phasenumwandlungen für einen untereutektoiden unlegierten Stahl*, Berichte aus der Technomathematik, FB 3, Universität Bremen, Report 0604, <http://www.math.uni-bremen.de/zetem/>, 2006.
48. M. WOLFF, M. BÖHM, D. HELM, *Material behaviour of steel – modelling of complex phenomena and investigations on thermodynamic consistency*, in press Int. J Plasticity, 2007.
49. M. WOLFF, S. BOETTCHER, M. BÖHM, *Phase transformations in steel in the multi-phase case – general modelling and parameter identification*, Berichte aus der Technomathematik, FB 3, Universität Bremen, Report 0702, <http://www.math.uni-bremen.de/zetem/>, 2007.
50. M. WOLFF, S. BOETTCHER, M. BÖHM, I. LORESCH, *Vergleichende Bewertung von makroskopischen Modellen für die austenitisch-perlitische Phasenumwandlung beim Stahl 100Cr6*, Berichte aus der Technomathematik, Report 07–03, University of Bremen, Germany, <http://www.math.uni-bremen.de/zetem/>, 2007.
51. E. ZEIDLER, *Nonlinear functional analysis and its applications IV – applications to mathematical physics*, Springer, 1997.
52. T. I. ZOHDI, P. WRIGGERS, *Introduction to Computational Micromechanics*, Springer, 2005.

Received December 13, 2006; revised version July 2, 2007.
